pubs.acs.org/Biomac

Article

Metal-Free Polymer-Based Affinity Medium for Selective Purification of His6-Tagged Proteins

Keiichi Yoshimatsu, Krista R. Fruehauf, Quanhong Zhu, Adam Weisman, Jun Fan, Min Xue, John M. Beierle, Paul E. Rose, Jennifer Aral, Linda F. Epstein, Philip Tagari, Les P. Miranda, and Kenneth J. Shea*

Cite This: *Biomacromolecules* 2021, 22, 1695−1705

Read Online

ACCESS | Metrics & More | Article Recommendations | Supporting Information

ABSTRACT: We report a metal free synthetic hydrogel copolymer with affinity and selectivity for His6-tagged peptides and proteins. Small libraries of copolymers incorporating charged and hydrophobic functional groups were screened by an iterative process for His6 peptide affinity. The monomer selection was guided by interactions found in the crystal structure of an anti-His tag antibody-His6 peptide antigen complex. Synthetic copolymers incorporating a phenylalanine-derived monomer were found to exhibit strong affinity for both His6-containing peptides and proteins. The proximity of both aromatic and negatively charged functional groups were important factors for the His6 affinity of hydrogel copolymers. His6 affinity was not compromised by the presence of enzyme cleavage sequences. The His6−copolymer interactions are pH sensitive: the copolymer selectively captured His6 peptides at pH 7.8 while the interactions were substantially weakened at pH 8.6. This provided mild conditions for releasing His6-tagged proteins from the copolymer. Finally, a synthetic copolymer coated chromatographic medium was prepared and applied to the purification of a His6-tagged protein from an *E. coli* expression system. The results establish that a synthetic copolymer-based affinity medium can function as an effective alternative to immobilized metal ion columns for the purification of His6-tagged proteins.

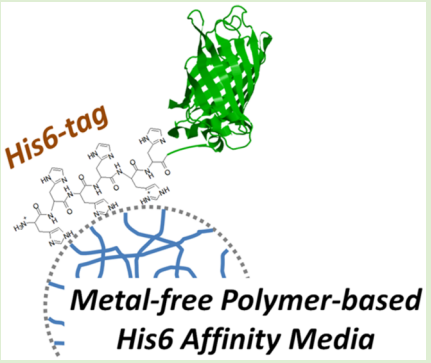

INTRODUCTION

Recombinant proteins occupy an essential role in modern biological science and biotechnology. They have revolutionized areas of research ranging from enzyme engineering for technical applications[1] to new therapies for human diseases.[2−4] To meet these expanding needs, recombinant proteins are now produced using a number of expression systems.[5,6] Regardless of the expression system, the production and purification of recombinant proteins are intimately linked. Indeed, the isolation and purification protocols are as important as the expression step itself.[7,8] Fusing an affinity tag at the N- or C-terminus of the recombinant protein is one of the techniques that have been widely used to streamline purification,[9−11] improve protein yields,[12,13] prevent proteolysis,[14] facilitate protein refolding,[15] reduce/increase antigenicity,[16] and/or increase solubility.[17−21] However, the physical properties and stability of the product proteins often restricts the conditions for separation and purification. The absence of a "one-size-fits-all" solution continues to drive the development of new separation and purification options.[9−11,22−25]

The polyhistidine-tag appended to the N- or C-terminus of a protein is one of the most common affinity tags in use. The presence of multiple imidazole groups, often six histidine residues (His6), allows for coordination to transition metal ions (e.g., Ni^{2+}, Co^{2+}, Cu^{2+}, Zn^{2+}) immobilized with a tetradentate ligand, nitrilotriacetic acid (NTA), attached to a solid support. This system, immobilized metal ion affinity chromatography (IMAC),[26] has proven to be extremely serviceable for affinity purification. The value of His-tags is derived in part from their small size; the presence of the tag exerts little disruptive effect on protein expression and folding.[27] The His-tag is broadly compatible with many proteins and is often proceeded by an enzymatically cleavable group for removal.[28] However, IMAC is not without some drawbacks. Histidine-rich proteins can coordinate with the immobilized metals on the column and coelute with the protein of interest.[25,29] Problems can also arise when purifying metalloproteins on IMAC columns due to the potential risk for metal removal or exchange with the metal on the column.[30] His-tagged proteins are frequently released from the solid support by treatment with high concentrations of imidazole which often necessitates an additional cleanup step.

Received: January 29, 2021
Revised: March 16, 2021
Published: March 30, 2021

https://doi.org/10.1021/acs.biomac.1c00119
Biomacromolecules 2021, 22, 1695−1705

Other studies have incorporated the basic concepts of IMAC into synthetic polymers by utilizing NTA as a comonomer.[31,32] However, these designs do not move away from the aforementioned issues associated with IMAC. There are commercially available anti-His tag antibodies but antibody-immobilized columns are more costly than IMAC columns.

Along those lines, our goal was to develop a metal-free, effective His-tag affinity material that could be used in place of IMAC. The work builds upon our synthetic antibody program that develops low information content statistical copolymers engineered with high affinity and selectivity for peptides and proteins.[33,34] Here we describe an *N*-isopropylacrylamide (NIPAm)-based, metal-free synthetic copolymer with affinity and selectively for His6-tagged peptides and proteins. We achieved this goal by incorporating both carboxylic acid and hydrophobic groups in the hydrogel copolymer. The highest His6-tag affinity copolymer incorporates an amino acid derived comonomer, *N*-acryloyl phenylalanine (AcPhe). The performance of the hydrogel copolymer as a chromatographic medium is demonstrated by coating a support material with the copolymer and comparing performance with an IMAC column for the purification of a His6-tagged protein from *E. coli* cell lysates at pH 7.8.

MATERIALS AND METHODS

Materials. All chemicals were obtained from commercial sources: propargylamine, *N*-isopropylacrylamide (NIPAm), *N*-phenylacrylamide (PAm), ammonium persulfate, sepharose CL-4B, epichlorohydrin, tris(hydroxymethyl)aminomethane (Tris), and glycine were from Sigma-Aldrich, Inc. (St. Louis, MO); β-mercaptoethanol (βME) and dimethyl sulfoxide (DMSO) were from Sigma, Ltd.; L-alanine, L-leucine, acrylic acid (AAc), and sodium dodecyl sulfate (SDS) were from Aldrich Chemical Co.; *N*,*N*′-methylenebis(acrylamide) (BIS) was from Fluka; *N*-*tert*-butylacrylamide (TBAm), sodium L-ascorbate, and ethylenediaminetetraacetic acid (EDTA) were from Acros Organics (Geel, Belgium); acryloyl chloride (96%, stabilized with 400 ppm phenothiazine) was from Alfa Aesar (Haverhill, MA); L-phenylalanine was from MP Biomedicals (Santa Ana, CA); sodium azide and sodium hydroxide (NaOH) were from Fisher Scientific; cupper (II) sulfate ($CuSO_4$) was from Mallinckrodt; and glycerol was from Merck KGaA (Darmstadt, Germany).

All peptides were synthesized by solid-phase peptide synthesis. Enhanced green fluorescence protein with hexahistidine tag (EGFP-His6) and insulin-like growth factor 1 receptor kinase domain with hexahistidine tag (His6-IGF1RKD) were recombinantly expressed in *E. coli*. After cell lysis, the proteins were purified by using immobilized ion affinity chromatography. The purified proteins were stored in 20 mM Tris-HCl Buffer (pH 8.0) containing 150 mM NaCl and 15% Glycerol at 4 °C until use. Protein Assay Kit, Precast SDS-PAGE gels (12% Mini-PROTEAN TGX) and a molecular weight marker solution (Precision plus protein standards) were purchased from Bio-Rad Laboratories, Inc. (Hercules, CA). NIPAm was recrystallized from hexane before use. Other chemicals were used as-received. Water used in polymerization and characterization was purified using a Barnstead Nanopure Diamond system.

Synthesis of *N*-Acryloyl L-Phenylalanine (AcPhe). *N*-Acryloyl L-phenylalanine was synthesized following a previously reported procedure.[35] L-Phenylalanine (3.63 g, 0.020 mol) was dissolved in 20 mL of 2 M sodium hydroxide aqueous solution. To a well-stirred aqueous solution of L-phenylalanine and sodium hydroxide, acryloyl chloride (1.75 mL, 0.022 mol) was added dropwise while the reaction mixture was kept below 0 °C by external ice-bath cooling. After the addition, stirring was continued for an additional 2 h at room temperature. The mixture was acidified to pH 2 with hydrochloric acid solution. A white product was separated by suction filtration and purified by recrystallization from water. Yield: 45.7% (2.74 g); ^{1}H NMR (500 MHz, CD_3OD) δ 7.27~7.16 (m, 5 H, C_6H_5), 6.27~6.13 (dd, J = 17.5 Hz, 10.5 Hz, 1 H, C*H*═CH_2), 6.21~6.13 (d, J = 17.5 Hz, 1 H, CH═C$H_{2\ trans}$), 5.62 (d, J = 10.5 Hz, 1 H, CH═C$H_{2\ cis}$), 4.75~4.71 (m, C*H*CH_2), 3.25~3.20 (m, 1 H, CH_2CH), 3.01~2.96 (m, 1 H, CH_2CH). ^{13}C NMR (125 MHz, CD_3OD) δ 173.18, 166.49, 137.02, 130.18, 128.83, 128.04, 126.41, 125.85, 53.78, 37.02; HRMS (ESI-TOF): m/z calcd for $C_{12}H_{13}NNaO_3$ $[M + Na]^+$ 242.0788; found 242.0790.

Synthesis of *N*-Acryloyl L-Leucine (AcLeu). L-Leucine (2.62 g, 0.020 mol) was dissolved in 20 mL of 2 M sodium hydroxide aqueous solution. To a well-stirred aqueous solution of L-leucine and sodium hydroxide, acryloyl chloride (1.75 mL, 0.022 mol) was added dropwise while the reaction mixture was kept below 0 °C by external ice-bath cooling. After the addition, stirring was continued for additional 2 h. The mixture was washed with ether. The mixture was acidified to pH 2 with hydrochloric acid solution. The white semisolid was collected by filtration. After the obtained semisolid was dissolved with preheated water and passed through a filter membrane. The filtrate was cooled down to yield a white product. Yield: 52.4% (1.94 g); ^{1}H NMR (500 MHz, CD_3Cl_3): δ 6.85 (d, J = 8.0 Hz, 1 H, N*H*), 6.28 (d, J = 16.5 Hz, 1 H, CH═C$H_{2\ trans}$), 6.19 (dd, J = 17.0 Hz, 10.5 Hz, 1 H, C*H*═CH_2), 5.67 (d, J = 10.0 Hz, 1 H, CH═C$H_{2\ cis}$), 4.62 (m, 1 H, CH_2C*H*NH), 1.71 (m, 2 H, CH_3CH_2CH), 1.64~1.61 (m, 1 H, $(CH_3)_2$C*H*CH_2), 0.94 (m, 6 H, $(CH_3)_2$CH); ^{13}C NMR (125 MHz, CD_3Cl_3): δ 176.19, 166.02, 129.97, 127.99, 51.03, 41.22, 24.95, 22.84, 21.94. MS (ESI-TOF): m/z calcd for $C_9H_{16}NO_3$ $[M + H]^+$ 186.2282, found 186.25; calcd for $C_9H_{15}NNaO_3$ $[M + Na]^+$ 208.2101, found 208.25.

Synthesis of *N*-Acryloyl L-Alanine (AcAla). L-Alanine (1.78 g, 0.020 mol) was dissolved in 20 mL of 2 M sodium hydroxide aqueous solution. To a well-stirred aqueous solution of L-alanine and sodium hydroxide, acryloyl chloride (1.75 mL, 0.022 mol) was added dropwise while the reaction mixture was kept below 0 °C by external ice-bath cooling. After the addition, stirring was continued for additional 2 h at room temperature. The mixture was acidified to pH 2 with hydrochloric acid solution. A white product was gradually formed and separated by filtration. Yield: 41.9% (1.20 g); ^{1}H NMR (500 MHz, DMSO-d_6): δ 8.43 (d, J = 7.0 Hz, 1 H, N*H*), 6.32 (dd, J = 16.5 Hz, 10.5 Hz, 1 H, C*H*═CH_2), 6.13 (d, J = 16.5 Hz, 1 H, CH═C$H_{2\ trans}$), 5.64 (d, J = 10.5 Hz, 1 H, CH═C$H_{2\ cis}$), 4.31 (t, J = 7.5 Hz, 1 H, CH_3C*H*), 1.33 (d, J = 7.5 Hz, 1 H, CH_3CH); ^{13}C NMR (125 MHz, DMSO-d_6): δ 174.57, 164.72, 131.80, 126.14, 47.98, 17.71; MS (ESI-TOF): m/z calcd for $C_6H_{10}NO_3$ $[M + H]^+$ 144.1485, found 144.3; calcd for $C_6H_9NNaO_3$ $[M + Na]^+$ 166.1304, found 166.2.

Synthesis of *N*-Propargyl Acrylamide. *N*-Propargyl acrylamide was synthesized by following a previously reported procedure[36] with a minor modification. Propargylamine (0.64 mL, 10 mmol) was dissolved in 15 mL of 1 M sodium hydroxide aqueous solution. To a well-stirred aqueous solution of propargylamine and sodium hydroxide, acryloyl chloride (1.22 mL, 15 mmol) in 2 mL of dichloromethane was added dropwise while the reaction mixture was kept at 0 °C by external ice-bath cooling. After addition was complete, stirring was continued for an additional 2 h at room temperature. The product was extracted with 15 mL of EtOAc three times and dried over anhydrous $MgSO_4$. The solvent was removed on a rotary evaporator to yield a pale brown solid. Yield: 74% (814 mg); ^{1}H NMR (500 MHz, CD_3OD): δ 6.30 (dd, 1 H, J = 1.1, 16.9 Hz), 6.09 (dd, 1 H, J = 10.4, 16.9 Hz), 5.93 (br, 1 H), 5.67 (dd, 1 H, J = 1.2, 10.3 Hz), 4.11 (dd, 2 H, J = 2.6, 5.3 Hz), 2.23 (t, 1 H, J = 2.4 Hz); ^{13}C NMR (125 MHz, CD3OD): δ 165.4, 130.2, 127.6, 79.5, 72.0, 29.5; HRMS (CI-TOF): m/z calcd for C_6H_8NO $[M + H]^+$ 110.0600; Found 110.0623.

Preparation of Polymer Nanoparticles (NPs) Consisting of AAc, PAm, and/or TBAm as Comonomer(s). The procedure reported by Debord and Lyon was adapted to synthesize polymer nanoparticles (NPs).[37−39] AAc (X mol %), PAm (Y mol %), TBAm (Z mol %), NIPAm (98 − X − Y − Z mol %), BIS (2 mol %), and SDS (10 mg) were dissolved in water (50 mL) and the resulting solutions were filtered through a no. 2 Whatman filter paper. PAm or TBAm was dissolved in acetonitrile (0.6 mL) or ethanol (1 mL),

https://doi.org/10.1021/acs.biomac.1c00119
Biomacromolecules 2021, 22, 1695−1705

respectively, before addition to the monomer solution. The total monomer concentration was 65 mM. Nitrogen gas was bubbled through the reaction mixtures for 30 min. Following the addition of ammonium persulfate aqueous solution (30 mg in 500 μL of water), the prepolymerization mixture was sealed under nitrogen gas. Polymerization was carried out by inserting the round bottle flask containing prepolymerization mixture in an oil bath preset to 60 °C for 3 h. The polymerized solutions were purified by dialysis using a dialysis membrane (12 000−14 000 Da MWCO) against an excess amount of pure water (changed more than twice a day) for 4 days. The NPs with a larger diameter were prepared in the identical manner except for omission of SDS. The prepared NPs could be stored at room temperature without noticeable change for several weeks.

Preparation of Polymer Nanoparticles Incorporating Amino Acid-Derived Comonomers. Amino acid-derived monomer (X mol %), NIPAm (98 − X mol %), BIS (2 mol %), and SDS (10 mg) were dissolved in water (50 mL) and the resulting solutions were filtered through a no. 2 Whatman filter paper. The total monomer concentration was 65 mM. Nitrogen gas was bubbled through the reaction mixtures for 30 min. Following the addition of ammonium persulfate aqueous solution (30 mg in 500 μL of water), the prepolymerization mixture was sealed under nitrogen gas. Polymerization was carried out by inserting the round-bottom flask containing prepolymerization mixture in an oil bath preset to 60 °C for 3 h. The polymerized solutions were purified by dialysis using a dialysis membrane (12 000−14 000 Da MWCO) against an excess of pure water (changed more than twice a day) for 4 days. The NPs with a larger diameter were prepared in the identical manner except for omission of SDS. The prepared NPs could be stored at room temperature without noticeable change for several weeks.

Characterization of NPs. The hydrodynamic diameter of NPs was determined in aqueous solution (25 ± 0.1 °C) by dynamic light scattering (DLS) instrument equipped with zetasizer software Ver. 6.12 (Zetasizer Nano ZS, Malvern Instruments, Ltd.). The yield and concentration of NPs were determined by gravimetric analysis of lyophilized aliquots of NPs.

Preparation of Polymer-Coated Sepharose CL-4B Beads. *Step i: Functionalization of Sepharose CL-4B beads*—Sepharose CL-4B (40 mL in gel volume) was washed with water (120 mL) 3× and then suspended in 25 mL of 1 M sodium hydroxide aqueous solution. Epichlorohydrin (20 mL, 0.25 mol) was added to the mixture. The pH of the gel suspension was ∼13. The mixture was incubated in an oil bath at 40 °C with vigorous stirring overnight. The gel was then thoroughly washed with Et_2O, acetone, and water. The number of epoxide groups in the epoxy-activated Sepharose was determined using the method of Sundberg and Porath.[40] Epoxy-activated Sepharose beads (100 μL gel volume) was added to 2 mL of 1.3 M sodium thiosulfate aqueous solution, and subsequently titrated with 1 M hydrochloric acid until pH 7.0 using phenol red as an indicator. The amount of hydrochloric acid consumed was used to estimate the number of epoxy groups on the Sepharose beads. The titration indicated that 1 mL (gel volume) of the functionalized Sepharose beads contain ∼0.04 mmol of epoxide groups. Sodium azide (4.5 g, 90 mmol) was dissolved in 100 mL of water and mixed with the epoxy-activated Sepharose beads (40 mL in gel volume). The mixture was incubated at room temperature with stirring overnight. The gel was thoroughly washed with water and kept in 10 mL water until further use. The azide-functionalized Sepharose beads (10 mL in gel volume, containing ∼0.4 mmol of azide groups) was suspended in 14 mL of methanol:water (1:1, v/v). To the suspension *N*-propargyl acrylamide (6.6 mg, 0.6 mmol) dissolved in 2.0 mL of methanol/water (1:1, v/v), 400 μL of 50 mM sodium ascorbate aqueous solution, and 100 μL of 100 mM $CuSO_4$ aqueous solution were added. The mixture was incubated at room temperature under stirring overnight. The gel was thoroughly washed once with water (200 mL), twice with 20 mM sodium phosphate buffer (pH 7.3) containing 1 mM EDTA (200 mL), twice with 20 mM sodium phosphate buffer (pH 7.3), and twice with water (400 mL). *Step ii: Coating of Sepharose CL-4B beads with polymer chains*—The propargyl acrylamide-functionalized Sepharose beads (5 mL in gel volume) was suspended in 10 mL of water containing monomers (AcPhe (40 mol %), NIPAm (58 mol %), and BIS (2 mol %)), 2 mg of sodium dodecyl sulfate, and 6 mg of ammonium persulfate. The total concentration of the monomers was 65 mM. The mixture was purged with dry nitrogen for 30 min and sealed under nitrogen. The reaction was initiated by inserting the flask into an oil bath at 60 °C and kept for 3 h with stirring. The polymer-coated Sepharose beads were then transferred in a plastic column with a frit and washed thoroughly with water. The prepared synthetic copolymer-coated beads could be stored at 4 °C (in a refrigerator) without noticeable change for several weeks.

Representative Procedure for the Quantification of Peptides Bound to NPs by Centrifugal Filtration Assay. Buffer solution (20 mM Tris-HCl (pH 7.8), 10% Tween 20 (w/v, in H_2O), peptide solution (100 μM in H_2O), and NP solution (6.0 mg mL^{-1} in H_2O) were prepared in separate tubes. The buffer solution (180.5 μL), 10% Tween 20 (2.5 μL), peptide solution (25 μL), and NP solution (42 μL) were mixed in centrifugal filtration tubes (Nanosep with Omega (modified poly(ether sulfone)) ultrafiltration membrane, MWCO: 100 kDa, PALL corp.) and incubated at room temp for 30 min. The final concentration of the buffer, peptide, and NP were ∼15 mM, 10 μM, and ∼1.0 mg mL^{-1}, respectively. Control samples had the NP solution replaced by an equal volume of purified water. In order to filter off the NPs and NP-bound peptides, the solution was passed through the membrane by the centrifugal filtration (10 000 rpm, 20 min, room temperature). Control samples had the NP solution replaced by an equal volume of purified water and were treated in the same manner as described above. A part of the filtrate (100 μL) was mixed with 100 μL of 4-acetamidobenzoic acid solution (40 μM in H_2O). The amount of the peptide present in the filtrate was quantified by HPLC (Solvents: A = H_2O + 0.1% TFA, B = MeCN + 0.1% TFA; Method: 0% B (5 min) → gradient (0% B to 50% B, over 10 min) → gradient (50% B to 100% B, over 1 min) → 100% B (5 min) → gradient (100% B to 0% B, over 1 min) → 0% B (5 min); Injection volume: 100 μL; Flow rate: 1.2 mL/min; Detection: absorbance at 220 nm.). The peak areas of the peptides were integrated and normalized against the peak area of the internal standard (4-acetamidobenzoic acid). The % of peptides bound to the NP was calculated by the following equation:

$$\%\mathrm{PBNP} = \left(1 - \frac{\mathrm{NPAPS}}{\mathrm{NPAPCS}}\right) \times 100$$

where %PBNP is the percentage of peptides bound to the NP, NPAPS is the normalized peak area of peptides in the sample, and NPAPCS is the normalized peak area of peptides in the control sample.

Procedure for Nonlinear Curve Fitting and Estimation of the Average Dissociation Constant of Binding Sites on AcPhe40 NP. The data of equilibrium binding study at different concentrations of AcPhe40 NPs for its ability to bind Met-His6-PreScission peptide in 15 mM Tris-HCl (pH 7.8) containing 0.1% Tween 20 were analyzed by nonlinear curve fitting with one-site model (eq 1).

$$B_{\mathrm{occupied}} = \frac{B_{\mathrm{max}} \times B_{\mathrm{unoccupied}}}{K_{\mathrm{d}} + B_{\mathrm{unoccupied}}} \quad (1)$$

In order to perform curve fitting, the amounts of peptide depleted from solution were used as B_{occupied} and the values calculated by the eq 2 were used as $B_{\mathrm{unoccupied}}$.

$$B_{\mathrm{unoccupied}} = x - B_{\mathrm{occupied}} \quad (2)$$

In each run, different values were assigned to x in eq 2, and the values for B_{max} and K_{d} that yield the best fit were computed by least-squares fitting regression analysis on Nonlinear Least Squares Curve Fitting Webtool.[41] The best estimate of x and K_{d} values for the binding sites with Met-His6-PreScission peptide affinity were determined from the fitting result that returned a value that was closest to 10 μmol binding sites/L of NP suspension, which corresponds to the theoretical maximum in this experimental setting, for B_{max}.

https://doi.org/10.1021/acs.biomac.1c00119
Biomacromolecules 2021, 22, 1695−1705

Procedure for Quantification of EGFPs Bound to NPs by Centrifugal Filtration Assay. Protein solution (80 μg mL^{-1} in 16 mM Tris-HCl (pH 7.8)), 10% Tween 20 (w/v, in H_2O), and NP solution (0.8 mg mL^{-1} in H_2O) were prepared in separate tubes. The protein solution (244.4 μL), 10% Tween 20 (2.5 μL), and NP solution (3.1 μL) were mixed in centrifugal filtration tubes (Nanosep with Omega (modified poly(ether sulfone)) ultrafiltration membrane, MWCO: 100 kDa, PALL Corp.) and incubated at room temp for 30 min. The final concentration of the protein and NP were ~8.0 μg mL^{-1} and 10 μg mL^{-1}, respectively. Control samples had the NP solution replaced by an equal volume of purified water. Centrifugation at 10 000 rpm at room temperature for 10 min filtered off the NPs and NP-bound proteins. Control samples replaced the NP solution by an equal volume of purified water and were treated in the same manner as described above. The amount of EGFPs in the filtrate was quantified by fluorescence measurements on SPEX Fluorolog spectrofluorometer (Jobin Yvon, Edison, NJ) (Excitation wavelength: 475 nm, and Emission wavelength: the average values of 497−500 nm.). The % of EGFPs bound to the NPs was calculated by the following equation:

$$\%\ \text{of EGFPs bound to the NP} = \left(1 - \frac{\text{FEIS}}{\text{FEICS}}\right) \times 100$$

where FEIS is the fluorescence emission intensity in the sample and FEICS is the fluorescence intensity in the control sample.

Procedure for Quantification of IGF1RKD Bound to NPs by Centrifugal Filtration Assay. Protein solution (80 μg mL^{-1} in 18.2 mM Tris-HCl (pH 7.8)), 10% Tween 20 (w/v, in H_2O), and NP solution (0.8 mg mL^{-1} in H_2O) were prepared in separate tubes. The protein solution (216.5 μL), 10% Tween 20 (2.5 μL), and NP solution (31 μL) were mixed in centrifugal filtration tubes (Nanosep with Omega (modified poly(ether sulfone)) ultrafiltration membrane, MWCO: 100 kDa, PALL corp.) and incubated at room temp for 30 min. The final concentration of the protein and NP were ~8.0 μg mL^{-1} and 100 μg mL^{-1}, respectively. Control samples had the NP solution replaced by an equal volume of purified water. Centrifugation at 10 000 rpm at room temperature for 5 min resulted in the NPs and NP-bound proteins being filtered off. Control samples replaced the NP solution by an equal volume of purified water and were treated in the same manner as described above. The amount of IGF1RKD in the filtrate was analyzed by SDS-PAGE.

Chromatographic Purification of EGFP-His6 Using Polymer-Coated Agarose Beads. A Polyprep column (Bio-Rad) was packed with 500 μL (in gel vol.) of the polymer-coated Sepharose CL-4B beads. The column was pre-equilibrated with by applying 10 mL of loading buffer (20 mM Tris-HCl (pH 7.8)). The EGFP-His6 solution (0.225 mL), an *E. coli* cell lysate solution (1 mL) and loading buffer (18.3 mL) were mixed and loaded to the column. Subsequently, 10 mL of wash buffer (20 mM Tris-HCl (pH 7.8)) was applied to the column to remove proteins weakly bound to the column. Finally, EGFP-His6 was eluted with 20 mM Tris-HCl (pH 8.6) (4 mL × 1 time) followed by 20 mM Tris-HCl (pH 9.0) (4 mL × 4 times).

In order to compare the effectiveness of polymer-coated agarose beads with a commercially available immobilized metal ion affinity column, a mixture of EGFP-His6 (0.225 mL), *E. coli* lysate (1 mL), and 25 mM Tris-HCl buffer (pH 8.0) containing 0.5 M NaCl and 10 mM imidazole (18.3 mL) was prepared and loaded to a Polyprep column packed with 500 μL (in gel vol.) of His-Pur Ni^{2+}-NTA agarose beads (Thermo Scientific). In this experiment, 25 mM Tris-HCl buffer (pH 8.0) containing 0.5 M NaCl and 20 mM imidazole (10 mL) was applied to the column in the wash step and 25 mM Tris-HCl buffer (pH 8.0) containing 0.3 M NaCl and 150 mM imidazole (4 mL × 5 times) was used to elute EGFP-His6 from the column.

All fractions from loading, wash, and elution steps were analyzed by SDS-PAGE and fluorescence measurements on Gemini XPS fluorescence microplate reader (Molecular Devices, LLC, Sunnyvale, CA) (Excitation wavelength at 475 nm, emission wavelength at 505 nm with a cutoff filter for 495 nm).

SDS-PAGE Analysis. The filtrates from centrifugal filtration assays or fractions from chromatographic study (7 μL) were mixed with a sample preparation solution (7 μL; water (68 vol %), glycerol (20 vol %), 2-mercaptoethanol (12 vol %), Tris (66.7 mM), SDS (40 mg/mL), bromophenol blue (0.04%, w/v)) and heated at 90 °C for 5−10 min. The prepared samples (10 μL) or molecular weight marker solution (0.7 μL) were loaded into the wells in 12% SDS-PAGE gels immersed in a running buffer (aqueous solution containing 25 mM Tris, 192 mM glycine and 0.1% SDS), separated by electrophoresis. The gels were stained using the silver staining method.

RESULTS AND DISCUSSION

Functional Group Selection, Copolymer Synthesis, and His6 Affinity Screen. The study begins with the synthesis of a small library of NIPAm copolymer NPs containing variable levels of negatively charged and hydrophobic comonomers. NPs of this type have been previously reported to exhibit high water content and mesh sizes sufficient to incorporate peptides and proteins into their interior.[33] We used directed chemical evolution, a method described previously for the discovery of synthetic copolymer complements to biological macromolecules.[34,42,43,38,44,45] The selection of monomers for inclusion in the copolymer was aided by analysis of the crystal structure of an anti-His tag antibody-His6 peptide antigen complex.[46] As shown in Figure 1, the

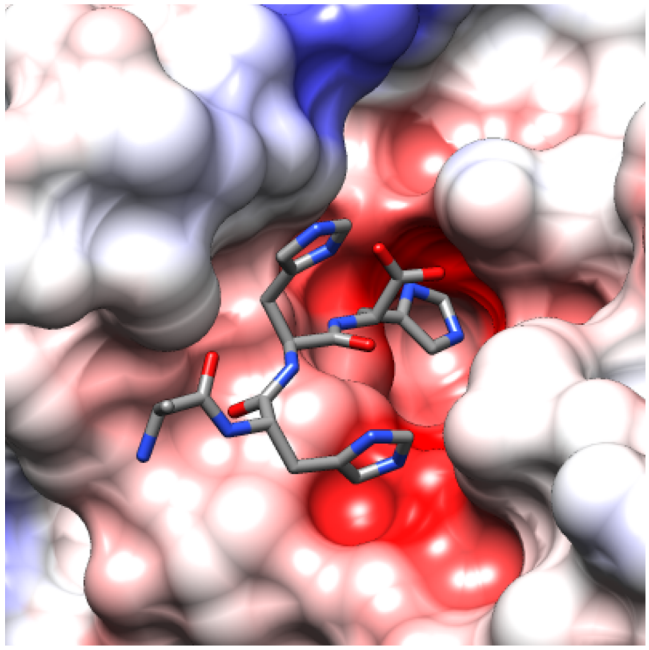

Figure 1. Binding pocket of anti-His tag antibody and C-terminus of His6 peptide antigen in the crystal structure of the antibody (PDB entry: 1KTR).[46] The negative and positive Coulombic potentials on the antibody surface are colored with red and blue, respectively. The peptide is colored by atom type C (gray), N (blue), and O(red).

binding pocket of the antibody consists predominantly of negatively charged areas and a nonpolar domain. Hydrophobic interactions are observed mainly between aromatic side chains of the antibody (Tyr, Phe) and the imidazole rings of the antigen. Additional hydrophobic interactions are observed between the aromatic ring of Phe and the main-chain atoms of His6 antigen. Acidic side chains in the binding cleft of the antibody provide a strong negative surface potential. The charged groups act as hydrogen bond acceptors for the nitrogen-protons of the antigen imidazole side chains. With this information, we synthesized a library incorporating varying

https://doi.org/10.1021/acs.biomac.1c00119
Biomacromolecules 2021, 22, 1695−1705

Table 1. Polymer NPs Used in the First Round of Screening[a]

polymer NP	AAc(mol %)	PAm(mol %)	TBAm(mol %)	NIPAm(mol %)	BIS(mol %)	D_H[b] (nm)
AAc5/PAm20	5	20		73	2	127
AAc5/PAm40	5	40		53	2	108
AAc20/PAm20	20	20		58	2	100
AAc20/PAm40	20	40		38	2	74
AAc5/TBAm40	5		40	53	2	85
AAc20/TBAm40	20		40	38	2	74
PAm20		20		78	2	109
PAm40		40		58	2	85
TBAm40			40	58	2	75
NIPAm				98	2	431

[a]The mol % of each monomer is in the feed ratio. [b]Hydrodynamic diameter of NPs determined by dynamic light scattering measurement.

amounts of acrylic acid (AAc) and *N*-*tert*-butylacrylamide (TBAm) or *N*-phenylacrylamide (PAm) monomers into NIPAm-based NPs. Ammonium persulfate was used as an initiator and all polymerization reactions were carried out in unbuffered aqueous solution at 60 °C. In order to control the size of NPs, a small amount of sodium dodecyl sulfate (SDS, 0.2 mg/mL) was also added to the polymerization mixture. AAc was selected as the carboxylic acid-containing comonomer for its hydrogen bond forming properties and negative charge near physiological pH (pH 7.8).[47,48] The aliphatic and aromatic hydrophobic comonomers, TBAm and PAm, were used to evaluate their relative effectiveness for binding to the His-rich peptide. The library was then screened for binding to a **Met-His6-PreScission** peptide (MHHHHHHLEVLFQGP-$CONH_2$). This peptide contains a common combination of N-terminus His6-tag and cleavage site of PreScission protease (LEVLFQGP).[28] Since many proteins have narrow stability windows, we desired to develop an affinity material that functioned as close to the physiological pH as possible. The monomer compositions of the NPs that were used in this work are summarized in Table 1.

The binding of **Met-His6-PreScission** peptide to the library of NPs in 15 mM Tris-HCl buffer containing 0.1% Tween 20 (w/v) was evaluated by incubation of NPs (1000 μg/mL) and peptides (10 μM) in buffer at room temperature followed by centrifugal filtration (Table 2). Unbound peptides in the filtrates were quantified using HPLC (Figure 2). The addition of 0.1% Tween 20 was necessary to mitigate the adsorption of peptides on the size exclusion membrane. The results establish that AAc incorporation is required for measurable levels of peptide binding. It was also found that NPs containing both PAm and AAc (**AAc5/PAm20**, **AAc20/PAm20**, and **AAc20/PAm40 NPs**) are more effective at binding to His6-PreScission peptide compared to the NPs containing comparable amounts of TBAm and AAc. This suggests that an aromatic hydrophobic functional group may be advantageous for affinity of His6-tags, a finding consistent with the antibody-His6 antigen complex structure analysis described above.[46]

Table 2. Peptide Sequences Used in This Study

peptide	sequence
Met-His6-PreScission	M**HHHHHH**LEVLFQGP-$CONH_2$
His6-PreScission	**HHHHHH**LEVLFQGP-$CONH_2$
His4-PreScission	**HHHH**LEVLFQGP-$CONH_2$
His2-PreScission	**HH**LEVLFQGP-$CONH_2$
Met-His6-TEV	M**HHHHHH**ENLYFQG-$CONH_2$
Met-His6-Caspase3	M**HHHHHH**DEVD-$CONH_2$

In contrast, polymer NPs that contain only hydrophobic monomers (TBAm or PAm) did not adsorb **Met-His6-PreScission** peptide. Among the screened NPs, **AAc20/PAm20** and **AAc20/PAm40 NPs** showed the highest binding capacity for **Met-His6-PreScission**. For example, **AAc20/PAm40 NPs** (250 μg in 250 μL solution) bound 2.83 μg out of the 4.63 μg of peptides originally added to the solution, ~60% of the total. The result suggests aromatic hydrophobic groups and anionic carboxylic acid groups participate cooperatively in **Met-His6-PreScission** peptide binding at pH 7.8. We also observe that the ratio of these two functional groups is important. For example, changing from AAc5/PAm20 to AAc20/PAm20 and from AAc5/PAm40 to AAc20/PAm40 produce significant increases in peptide binding. In both cases, the change in ratio has a significant effect on peptide binding. Although these trends suggest further optimization, we point out that we are unable to explore all compositional space because of concern with the stability of NPs in aqueous solution. Although the data may suggest further increasing PAm content, our previous study showed that at high hydrophobic monomer content one encounters NP instability and/or clustering of hydrophobic groups within the NP, compromising their effectiveness for interacting with peptides or proteins.[40]

Contribution of Amino Acid-Derived Bifunctional Comonomers to His6 Binding. Negatively charged and hydrophobic groups were found to be important for binding to **Met-His6-PreScission** peptide. Within the synthetic copolymer, these two functional groups are statistically distributed throughout the polymer network. These same functional groups are also responsible for binding in the antibody-His6 peptide complex, but in the protein−peptide complex the two groups can be found in close proximity. Indeed, the presence of charged and hydrophobic groups in close proximity is a structural motif found in many "hot spots" sites where alanine mutations cause a significant increase in binding free energy (greater than 2 kcal/mol).[49,50] To evaluate if proximity of hydrophobic and charged groups could result in enhanced binding, we examined the effect of amino acid-derived bifunctional comonomers containing both groups within a single monomer unit.[51,35,52] To this point, we synthesized and evaluated a small library of polymer NPs that incorporated three amino acid-derived comonomers, *N*-acryloyl phenylalanine (AcPhe), *N*-acryloyl leucine (AcLeu), and *N*-acryloyl alanine (AcAla). The size and nature of the hydrophobic group was of particular interest, thus a phenyl group, isobutyl group,

https://doi.org/10.1021/acs.biomac.1c00119
Biomacromolecules 2021, 22, 1695−1705

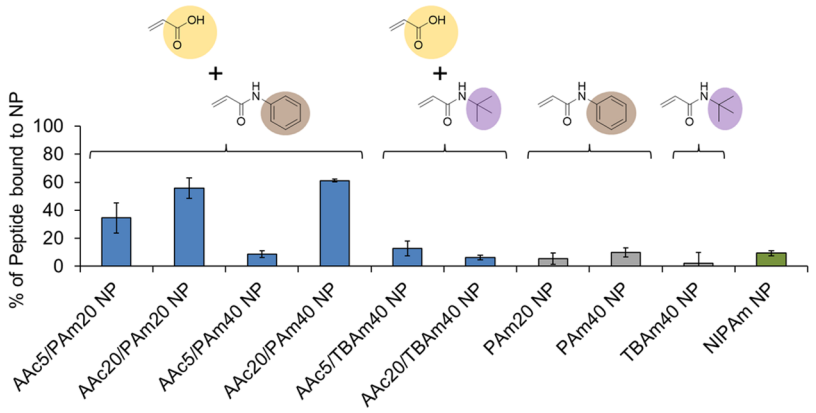

Figure 2. Binding of **Met-His6-PreScission** peptide (MHHHHHHLEVLFQGP-$CONH_2$) to polymer NPs incorporating various comonomers in 15 mM Tris-HCl buffer (pH 7.8) containing 0.1% Tween 20 (w/v). Concentration of peptide = 10 μM (18.55 μg/mL). Concentration of polymer nanoparticles = 1000 μg/mL.

Table 3. Polymer NPs Used in the Second Round of Screening[a]

polymer NP	AcPhe(mol %)	AcLeu(mol %)	AcAla(mol %)	NIPAm(mol %)	BIS(mol %)	D_H[b] (nm)
AcPhe20	20			78	2	106
AcPhe40	40			58	2	94
AcLeu20		20		78	2	81
AcLeu40		40		58	2	76
AcAla20			20	78	2	817
AcAla40			40	58	2	1232

[a]The mol % of each monomer is in the feed ratio. [b]Hydrodynamic diameter of NPs determined by dynamic light scattering measurement.

and methyl group were compared in this series. The composition of these copolymers can be found in Table 3.

As shown in Figure 3, the polymer NP incorporating 40 mol % of AcPhe (**AcPhe40 NP**) was identified as the most effective candidate. This NP absorbs >90% of the peptide added. NPs incorporating 20 mol % of AcPhe comonomer (**AcPhe20 NP**), 40 mol % of AcLeu comonomer (**AcLeu40 NP**) or AcAla comonomer (**AcAla40 NP**) absorbed less than 50% of the peptides added to the solution. It is clear the importance of proximity of charged and aromatic functional groups.

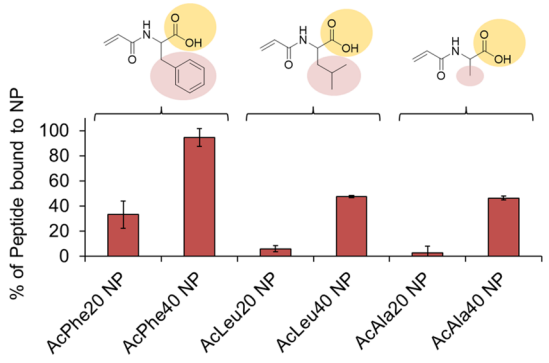

Figure 3. Binding of **Met-His6-PreScission** peptide (MHHH-HHHLEVLFQGP-$CONH_2$) to polymer NPs incorporating 20 mol % or 40 mol % of AcPhe, AcLeu, or AcAla comonomers in 15 mM Tris-HCl buffer (pH 7.8) containing 0.1% Tween 20 (w/v). Concentration of peptide = 10 μM (18.55 μg/mL). Concentration of polymer NPs = 1000 μg/mL.

In an effort to compare **AcPhe40 NP** and a previously reported anti-His tag antibody single-chain variable fragment (scFv), we performed a nonlinear curve fitting analysis of the binding curve (Figure S1 of the Supporting Information, SI). The curve fitting analysis gave 14.7 nmol binding sites/mg polymer and ~300 nM as the estimated values for the number of the binding sites and average K_d reported anti-His tag antibody 3D5 scFv binds the His-tagged peptide with a K_d of nmol His tag peptide/mg of scFv. Therefore, despite the fact that these synthetic materials present a range of affinities, the ensemble of binding sites on **AcPhe40 NP** exhibits a performance that is comparable to its antibody counterpart in terms of the numbers of binding sites (per weight basis) and average affinity of the binding sites.

To investigate the correlation between the number of consecutive histidine residues and the binding affinity as a function of the AcPhe comonomer percentage, the binding of three linear peptides, **His6-PreScission**, **His4-PreScission**, and **His2-PreScission** containing six, four, or two histidine residues with a protease cleavage site, were tested against **AcPhe40** and **AcPhe20 NPs.** A polymer NP that does not contain the AcPhe comonomer was also included. As seen in Figure 4, binding tracks with increasing histidine residues especially as the content of AcPhe in NPs increased. This result clearly demonstrates that the histidine residues are the major contributors to NP binding. Additionally, interactions[53,54] between multiple imidazole rings and the NP functional groups are important for strong NP-peptide binding. It is noteworthy that anti-His tag antibody 3D5 binds with His6, His4, and His3 peptides with equal strength.[46] In contrast, **AcPhe40 NP** binds more strongly with His6 peptide compared to His4, suggesting that the **AcPhe40 NP** interacts with a longer stretch of histidine residues than the biological antibody counterpart.

In some cases, the His6-tags are removed before the target can be characterized or applied. Conventional methods include tag removal by highly specific proteases.[28] The preceding results showed that the **AcPhe40** and **AcPhe20 NPs** exhibit

https://doi.org/10.1021/acs.biomac.1c00119
Biomacromolecules 2021, 22, 1695−1705

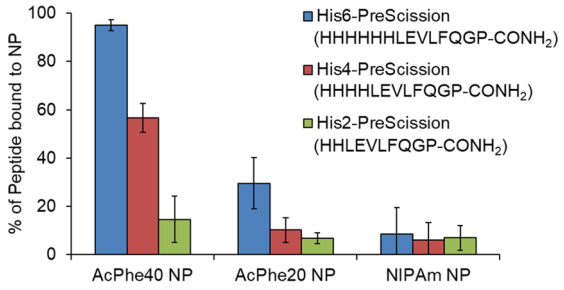

Figure 4. Binding of peptides containing different numbers of histidine residues to **AcPhe40**, **AcPhe20**, and **NIPAm NPs** that incorporate 40 mol %, 20 mol %, and 0 mol % of AcPhe comonomer, respectively, in 15 mM Tris-HCl buffer (pH 7.8) containing 0.1% Tween 20 (w/v). Concentration of peptide = 10 μM (18.55 μg/mL). Concentration of polymer nanoparticles = 1000 μg/mL.

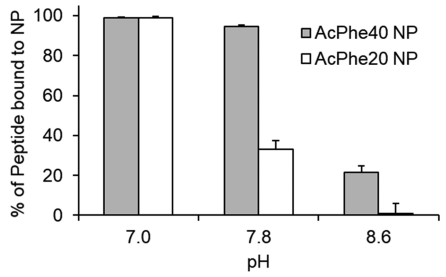

Figure 5. Binding of **Met-His6-PreScission** (MHHHHHHLEVLFQGP-CONH$_2$) to **AcPhe40** and **AcPhe20 NPs** in 15 mM Tris-HCl buffer (pH 7.0, 7.8, or 8.6) containing 0.1% Tween 20 (w/v). Concentration of peptide = 10 μM (18.55 μg/mL). Concentration of polymer NPs = 1000 μg/mL.

strong affinity for the peptide containing the PreScission protease cleavage site. Since the protease cleavage sequence could affect the copolymer affinity to the His6 sequence, we compared binding of **AcPhe40 NP** to two additional common protease cleavage sequences fused with affinity tags, **Met-His6-TEV** (ENLYFQG) and **Met-His6-Caspase3** (DEVD). As shown in Table 4, **AcPhe40 NP** was effective for binding all three His6 containing peptides although **Met-His6-Caspase3** showed a slightly lower level of binding. This could be due to local electrostatic repulsions between the negative charges on **AcPhe40 NP** and the negative charges on aspartate and glutamate residues on the Caspase-3 cleavage site (DEVD) at pH 7.8. The cleavage sequences for PreScission protease (LEVLFQGP) and TEV protease (ENLYFQG) contain only 1 negatively charged residue and could account for the stronger NP binding of **Met-His6-PreScission** and **Met-His6-TEV** in comparison to **Met-His6-Caspase3**.

After establishing that the primary basis of **AcPhe40 NPs** affinity was the His6-tag, the conditions required for peptide release from the NPs were explored. In IMAC, elution of His-tagged proteins is often achieved by competitively displacing the His-tagged protein from immobilized metal-ions by high concentration (250 mM or higher) of imidazole. These conditions require a subsequent purification step. To circumvent this, we investigated if NP-His6 interactions can be altered by small changes in pH. It was found that an *increase* in pH is an effective means of weakening the copolymer−peptide interactions (Figure 5). At neutral pH (7.0), both **AcPhe40** and **AcPhe20 NPs** captured most of **Met-His6-PreScission** peptide in the solution. However, as the pH is increased slightly to 7.8, binding of **AcPhe20 NP** to the peptide falls off significantly. The affinity of **AcPhe40 NP** for the His6 peptide drops off at pH 8.6. We can use this pH responsiveness to trigger the release of captured proteins from the synthetic copolymer NPs.

The pH sensitivity may be attributed to the average number of positive charges on His6-tag. The pK_a of the histidine side chain is ∼6. The number of formal charges present in His6-tags can be roughly estimated to +0.6, + 0.095, and +0.015, respectively, at pH 7.0, 7.8, and 8.6. Thus, the His-tags lose their partial positive charge over a narrow range of pH. Although hydrophobic domains such as phenyl rings on AcPhe monomer units could interact with the imidazole ring via $\pi-\pi$ interactions, without electrostatic interactions with the anionic carboxylic acid, the affinity is weakened. This explanation appears to be consistent with the pH responsivity of the anti-His tag antibody 3D5 single-chain fragment.[55]

Binding of His6-Tagged Proteins to AcPhe40 NPs. The goal of this work was to develop an effective metal-free affinity medium for purification of His6-tagged proteins from protein expression systems. **AcPhe40 NP** was the most promising candidate. We chose enhanced green fluorescence protein (EGFP) and insulin-like growth factor 1 receptor kinase domain (IGF1RKD) for this study. Both expressed proteins were fused with His6-tags. A centrifugal filtration assay procedure was used to evaluate the polymer NP−peptide interactions for this study. As shown in Figures 6 and 7 both

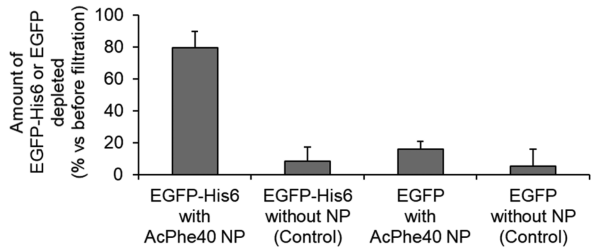

Figure 6. Result of centrifugal filtration assay for evaluating the binding of EGFP-His6 to **AcPhe40 NP** in 15 mM Tris-HCl buffer (pH 7.8) containing 0.1% Tween 20 (w/v) and subsequent centrifugal filtration. Concentration of protein (EGFP-His6 or EGFP) = 8 μg/mL (0.24 μM). Concentration of **AcPhe40 NP** = 10 μg/mL.

Table 4. Binding of His6 Containing Peptides Fused with Different Protease Cleavage Sequences to AcPhe40 NP in 15 mM Tris-HCl Buffer (pH 7.8) Containing 0.1% Tween 20 (w/v)[a]

peptide	sequence	% peptide bound to AcPhe40 NP
Met-His6-PreScission	MHHHHHHLEVLFQGP-CONH$_2$	94.5 ± 0.8%
Met-His6-TEV	MHHHHHHENLYFQG-CONH$_2$	96.4 ± 3.2%
Met-His6-Caspase	MHHHHHHDEVD-CONH$_2$	72.1 ± 7.2%

[a]Concentration of peptide = 10 μM. Concentration of polymer nanoparticles = 1000 μg/mL.

https://doi.org/10.1021/acs.biomac.1c00119
Biomacromolecules 2021, 22, 1695−1705

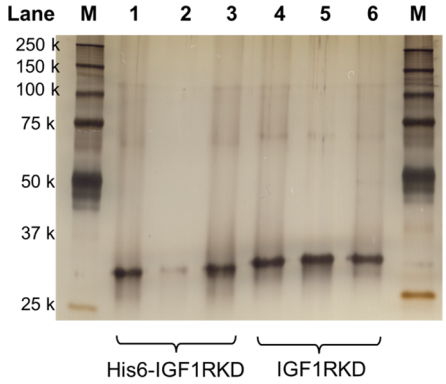

Figure 7. SDS-PAGE analysis of filtrates from the centrifugal filtration assay for evaluating the binding of His6-IGF1RKD to **AcPhe40 NP** in 15 mM Tris-HCl buffer (pH 7.8) containing 0.1% Tween 20 (w/v). Concentration of protein (His6-IGF1RKD or IGFRKD) = 8 μg/mL (0.24 μM). Concentration of **AcPhe40 NP** = 100 μg/mL. Lanes M: molecular weight markers. Lane 1: His6-IGF1RKD-His6 control (without filtration). Lane 2: His6-IGF1RKD + **AcPhe40 NP** (filtrate). Lane 3: His6-IGF1RKD without NP (filtrate). Lane 4: IGF1RKD control (without filtration). Lane 5: IGF1RKD + **AcPhe40 NP** (filtrate). Lane 6: IGF1RKD without NP (filtrate). The gel image was taken after silver staining.

EGFP-His6 and His6-IGF1RKD were taken up by **AcPhe40 NP**. In contrast, neither EGFP nor IGF1RKD proteins lacking the His6-tag bound to **AcPhe40 NP**. Control experiments were carried out in the absence of polymer NPs confirmed that the depletion of proteins from solution was due to the absorption by the polymer NPs and not caused by adhesion to the filter membrane.

Chromatographic Purification of EGFP-His6. The use of the centrifugal filtration procedure allowed for demonstrating small scale (250 μL) capture of His6-tagged proteins. However, this procedure has limitations in terms of scalability. When the experiment is performed at higher NP concentrations or with larger sample volumes, the NPs clogged the pores on the filtration membrane after only a portion of the sample solution passed through the filtration unit. To overcome this problem, we prepared agarose beads coated with a layer of polymer chains consisting of the same monomer composition as **AcPhe40 NP** to evaluate the utility of the copolymer-coated agarose gels for isolating EGFP-His6 from other proteins that are derived from *E. coli* cells. The polymer-coated agarose beads were prepared by the introduction of covalently linked double bonds to the agarose beads via the introduction of epoxide group, azidation,[40] and copper-catalyzed "click" reaction,[56] followed by copolymerization of comonomers in the presence of modified beads. This procedure was developed to attach polymer chains to agarose beads without introducing any undesired charged groups. The result of elemental analysis indicated that at least 10% (in weight %) of the polymer-coated beads consists of copolymer chains (Table S2). His-Pur Ni^{2+}-NTA resin was used for a direct comparison with a commercially available affinity medium for Ni^{2+}-NTA-based IMAC.

Table 5 summarizes the result of the chromatographic study. In this study, a protein mixture sample containing *E. coli* cell lysate and EGFP-His6 were diluted in 20 mM Tris-HCl buffer (pH 7.8) and loaded on the column. After proteins loosely bound to the column were washed off with 20 mM Tris-HCl buffer (pH 8.0), EGFP-His6 was eluted by applying 20 mM

Table 5. Amount of EGFP-His6 Found in Each Fraction from the Chromatographic Study[a]

	amount of EGFP found (% vs loaded protein mixture sample)	
fraction	HisPur Ni-NTA	AcPhe40-coated Sepharose CL-4B
flow-through	3.1	2.4
wash	0.3	1.7
elution 1	23.7	38.1
elution 2	21.7	20.5
elution 3	14.6	13.8
elution 4	7.9	3.2
elution 5	5.3	2.4

[a]The amount of EGFP was determined based on the fluorescence intensity (Ex. 475 nm, Em. 505 nm, cutoff filter 495 nm) and volume of each fraction.

Tris-HCl buffer with slightly higher pH (pH 8.6 and 9.0). The amount of EGFP in each fraction was then determined by fluorescence measurements. The result showed the **AcPhe40**-coated Sepharose CL-4B column strongly retained the EGFP-His6 throughout the sample loading and wash steps. The elution condition used in this experiment allowed for recovery of up to 78% of EGFP-His6 from the AcPhe40-coated Sepharose CL-4B column. Figure 8 shows the SDS-PAGE

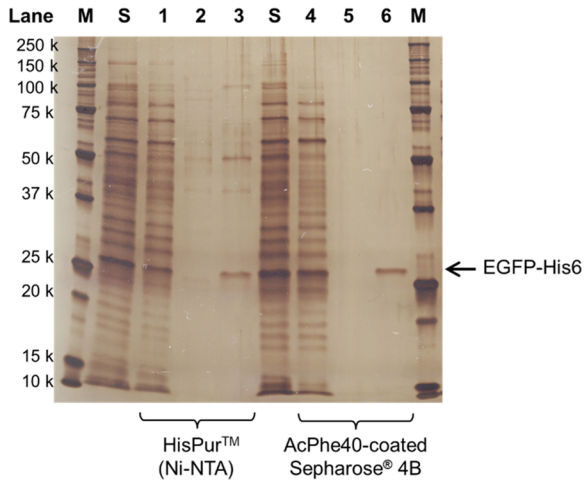

Figure 8. SDS-PAGE analysis of fractions from a chromatographic study. Lanes M: molecular weight markers. Lanes S: protein mixture sample prior to chromatographic separation. Lane 1: flow-through fraction from HisPur Ni-NTA column. Lane 2: wash fraction from HisPur Ni-NTA column. Lane 3: 1st to 3rd elution fractions from HisPur Ni-NTA column Three fractions were combined prior to the analysis. Lane 4: flow-through fraction from AcPhe40-coated Sepharose CL-4B column. Lane 5: wash fraction from AcPhe40-coated Sepharose CL-4B column. Lane 6: 1st to 3rd elution fractions from AcPhe40-coated Sepharose CL-4B column. Three fractions were combined prior to the analysis. The gel image was taken after silver staining.

analysis of flow-through, wash, and combined elution fractions 1−3. Most proteins derived from *E. coli* host cells were found in the flow-through fraction, and the elution fractions contained highly purified EGFP-His6. The result establishes that **AcPhe40**-coated Sepharose CL-4B beads are effective for separating EGFP-His6 from complex matrixes (*E. coli* cell lysates). The purity of recovered EGFP-His6 was comparable to or slightly higher than the sample purified by Ni^{2+}-NTA

https://doi.org/10.1021/acs.biomac.1c00119
Biomacromolecules 2021, 22, 1695−1705

agarose beads. Overall, fluorescence measurements and SDS-PAGE analysis showed that **AcPhe40**-coated Sepharose CL-4B column functions as effectively as a Ni-NTA column (HisPur) demonstrating the practical utility of the **AcPhe40** copolymer.

CONCLUSIONS

A metal-free, selective affinity material for the His6-tag has been developed. The material, a hydrogel copolymer, was identified from a screen of small libraries of hydrogel copolymer NPs. The choice of comonomers for the polymer libraries was guided by analysis of the X-ray crystal structure of the anti-His tag antibody 3D5 single-chain fragment complexed to its antigen. The structural biology study indicated both negatively charged and hydrophobic groups would be important for affinity to the His6 antigen. Initial screening of synthetic polymer-based NPs showed that NPs incorporating both acrylic acid (AAc) and *N*-phenylacrylamide (PAm) exhibit moderate His6-tag affinity. Further refinement incorporating bifunctional amino acid-derived monomers revealed that the proximity of both aromatic group and negative charge in a phenylalanine-derived monomer was found to be most effective. A lightly cross-linked NIPAm based hydrogel copolymer incorporating 40% of *N*-acryloyl phenyl alanine (**AcPhe40**), exhibited high affinity for both His6-tagged peptides and proteins in 15 mM Tris-HCl buffer at pH 7.8. Affinity was relatively insensitive to the inclusion of enzyme cleavage sequence. It was also found that the His6-tag affinity of **AcPhe40 NP** is pH sensitive and is substantially weakened at pH 8.6. The pH responsiveness was used to release His6-tagged proteins from the copolymer. Column chromatography experiments with **AcPhe40**-coated agarose beads efficiently captured and released a His6-tagged EGFP (EGFP-His6) from *E. coli* cell lysate establishing the potential synthetic polymer-based affinity materials for purification of His6-tagged proteins. The affinity material does not rely on metal-histidine coordination, and therefore offers potential advantages over IMAC.

ASSOCIATED CONTENT

Supporting Information

The Supporting Information is available free of charge at https://pubs.acs.org/doi/10.1021/acs.biomac.1c00119.

Procedure for NMR measurements, summary of NP characterization data, schematic illustration of steps in the preparation of polymer-coated Sepharose CL-4B beads, elemental analysis data, equilibrium binding curve of AcPhe40 NP for Met-His6-PreScission peptide, and ^{1}H and ^{13}C NMR spectra (PDF)

AUTHOR INFORMATION

Corresponding Author

Kenneth J. Shea − *Department of Chemistry, University of California, Irvine, California 92697, United States;* orcid.org/0000-0001-5926-0059; Email: kjshea@uci.edu

Authors

Keiichi Yoshimatsu − *Department of Chemistry, University of California, Irvine, California 92697, United States; Department of Chemistry, Missouri State University, Springfield, Missouri 65897, United States;* orcid.org/0000-0002-1428-0029

Krista R. Fruehauf − *Department of Chemistry, University of California, Irvine, California 92697, United States*

Quanhong Zhu − *Department of Chemistry, University of California, Irvine, California 92697, United States*

Adam Weisman − *Department of Chemistry, University of California, Irvine, California 92697, United States*

Jun Fan − *Department of Chemistry, University of California, Irvine, California 92697, United States;* orcid.org/0000-0003-2986-8551

Min Xue − *Department of Chemistry, University of California, Irvine, California 92697, United States;* orcid.org/0000-0001-9786-8225

John M. Beierle − *Department of Chemistry, University of California, Irvine, California 92697, United States*

Paul E. Rose − *Therapeutic Discovery, Amgen Inc., Thousand Oaks, California 91320, United States*

Jennifer Aral − *Therapeutic Discovery, Amgen Inc., Thousand Oaks, California 91320, United States*

Linda F. Epstein − *Therapeutic Discovery, Amgen Inc., Thousand Oaks, California 91320, United States*

Philip Tagari − *Therapeutic Discovery, Amgen Inc., Thousand Oaks, California 91320, United States*

Les P. Miranda − *Therapeutic Discovery, Amgen Inc., Thousand Oaks, California 91320, United States*

Complete contact information is available at: https://pubs.acs.org/10.1021/acs.biomac.1c00119

Notes

The authors declare no competing financial interest.

ACKNOWLEDGMENTS

We thank Prof. Charles G. Glabe (UCI) for providing access to a fluorescence microplate reader.

ABBREVIATIONS

AAc	acrylic acid
AcAla	*N*-acryloyl L-alanine
AcLeu	*N*-acryloyl L-leucine
AcPhe	*N*-acryloyl L-phenylalanine
BIS	*N,N′*-methylenebisacrylamide
EGFP	enhanced green fluorescence protein
IGF1RKD	insulin-like growth factor 1 receptor kinase domain
IMAC	immobilized metal ion affinity chromatography
NIPAm	*N*-isopropyl acrylamide
NP	nanoparticle
NTA	nitrilotriacetic acid
PAm	*N*-phenyl acrylamide
SDS	sodium dodecyl sulfate
TBAm	*N*-*tert*-butyl acrylamide

REFERENCES

(1) Arnold, F. H. Directed Evolution: Bringing New Chemistry to Life. *Angew. Chem., Int. Ed.* **2018**, *57*, 4143−4148.

(2) Leader, B.; Baca, Q. J.; Golan, D. E. Protein Therapeutics: A Summary and Pharmacological Classification. *Nat. Rev. Drug Discovery* **2008**, *7*, 21−39.

(3) Dimitrov, D. S. Therapeutic Proteins. In *Therapeutic Proteins: Methods and Protocols*; Voynov, V., Caravella, J. A., Eds.; *Methods Mol. Biol.*; Humana Press: Totowa, NJ, 2012; pp 1−26.

(4) Lagassé, H. A. D.; Alexaki, A.; Simhadri, V. L.; Katagiri, N. H.; Jankowski, W.; Sauna, Z. E.; Kimchi-Sarfaty, C. Recent Advances in (Therapeutic Protein) Drug Development. *F1000Research* **2017**, *6*, 113.

(5) Brondyk, W. H. Chapter 11. Selecting an Appropriate Method for Expressing a Recombinant Protein. In *Methods in Enzymology*; Burgess, R. R., Deutscher, M. P., Eds.; Guide to Protein Purification, 2nd ed.; Academic Press: New York, 2009; Vol. *463*, pp 131−147.
(6) Oliveira, C.; Domingues, L. Guidelines to Reach High-Quality Purified Recombinant Proteins. *Appl. Microbiol. Biotechnol.* **2018**, *102*, 81−92.
(7) Gronemeyer, P.; Ditz, R.; Strube, J. Trends in Upstream and Downstream Process Development for Antibody Manufacturing. *Bioengineering* **2014**, *1*, 188−212.
(8) Tripathi, N. K.; Shrivastava, A. Recent Developments in Bioprocessing of Recombinant Proteins: Expression Hosts and Process Development. *Front. Bioeng. Biotechnol.* **2019**, *7*, 240.
(9) Zhao, X.; Li, G.; Liang, S. Several Affinity Tags Commonly Used in Chromatographic Purification. *J. Anal. Methods Chem.* **2013**, *2013*, 581093.
(10) Waugh, D. S. Making the Most of Affinity Tags. *Trends Biotechnol.* **2005**, *23*, 316−320.
(11) Young, C. L.; Britton, Z. T.; Robinson, A. S. Recombinant Protein Expression and Purification: A Comprehensive Review of Affinity Tags and Microbial Applications. *Biotechnol. J.* **2012**, *7*, 620−634.
(12) Rajan, S. S.; Lackland, H.; Stein, S.; Denhardt, D. T. Presence of an N-Terminal Polyhistidine Tag Facilitates Stable Expression of an Otherwise Unstable N-Terminal Domain of Mouse Tissue Inhibitor of Metalloproteinase-1 In Escherichia Coli. *Protein Expression Purif.* **1998**, *13*, 67−72.
(13) Sun, Q.-M.; Chen, L.-L.; Cao, L.; Fang, L.; Chen, C.; Hua, Z.-C. An Improved Strategy for High-Level Production of Human Vasostatin120−180. *Biotechnol. Prog.* **2005**, *21*, 1048−1052.
(14) Tang, W.; Sun, Z.-Y.; Pannell, R.; Gurewich, V.; Liu, J.-N. An Efficient System for Production of Recombinant Urokinase-Type Plasminogen Activator. *Protein Expression Purif.* **1997**, *11*, 279−283.
(15) Kou, G.; Shi, S.; Wang, H.; Tan, M.; Xue, J.; Zhang, D.; Hou, S.; Qian, W.; Wang, S.; Dai, J.; Li, B.; Guo, Y. Preparation and Characterization of Recombinant Protein ScFv(CD11c)-TRP2 for Tumor Therapy from Inclusion Bodies in Escherichia Coli. *Protein Expression Purif.* **2007**, *52*, 131−138.
(16) Mayer, A.; Sharma, S. K.; Tolner, B.; Minton, N. P.; Purdy, D.; Amlot, P.; Tharakan, G.; Begent, R. H. J.; Chester, K. A. Modifying an Immunogenic Epitope on a Therapeutic Protein: A Step towards an Improved System for Antibody-Directed Enzyme Prodrug Therapy (ADEPT). *Br. J. Cancer* **2004**, *90*, 2402−2410.
(17) Chen, H.; Xu, Z.; Xu, N.; Cen, P. Efficient Production of a Soluble Fusion Protein Containing Human Beta-Defensin-2 in E. coli Cell-Free System. *J. Biotechnol.* **2005**, *115* (3), 307−315.
(18) Loughran, S. T.; Walls, D. Tagging Recombinant Proteins to Enhance Solubility and Aid Purification. In *Protein Chromatography: Methods and Protocols*; Walls, D., Loughran, S. T., Eds.; *Methods Mol. Biol.*; Springer: New York, NY, 2017; pp 131−156.
(19) Dyson, M. R.; Shadbolt, S. P.; Vincent, K. J.; Perera, R. L.; McCafferty, J. Production of Soluble Mammalian Proteins in Escherichia Coli: Identification of Protein Features That Correlate with Successful Expression. *BMC Biotechnol.* **2004**, *4*, 32.
(20) Hammarström, M.; Hellgren, N.; van den Berg, S.; Berglund, H.; Härd, T. Rapid Screening for Improved Solubility of Small Human Proteins Produced as Fusion Proteins in *Escherichia Coli*. *Protein Sci.* **2002**, *11*, 313−321.
(21) Nallamsetty, S.; Waugh, D. S. Solubility-Enhancing Proteins MBP and NusA Play a Passive Role in the Folding of Their Fusion Partners. *Protein Expression Purif.* **2006**, *45*, 175−182.
(22) Dias, A. M. G. C.; Roque, A. C. A. The Future of Protein Scaffolds as Affinity Reagents for Purification. *Biotechnol. Bioeng.* **2017**, *114*, 481−491.
(23) Wood, D. W. New Trends and Affinity Tag Designs for Recombinant Protein Purification. *Curr. Opin. Struct. Biol.* **2014**, *26*, 54−61.
(24) Pina, A. S.; Lowe, C. R.; Roque, A. C. A. Challenges and Opportunities in the Purification of Recombinant Tagged Proteins. *Biotechnol. Adv.* **2014**, *32*, 366−381.
(25) Rowinska-Zyrek, M.; Witkowska, D.; Potocki, S.; Remelli, M.; Kozlowski, H. His-Rich Sequences − Is Plagiarism from Nature a Good Idea? *New J. Chem.* **2013**, *37*, 58−70.
(26) Bornhorst, J. A.; Falke, J. J. Purification of Proteins Using Polyhistidine Affinity Tags. In *Methods Enzymol*; Applications of Chimeric Genes and Hybrid Proteins Part A: Gene Expression and Protein Purification; Academic Press: New York, 2000; Vol. *326*, pp 245−254.
(27) Carson, M.; Johnson, D. H.; McDonald, H.; Brouillette, C.; DeLucas, L. J. His-Tag Impact on Structure. *Acta Crystallogr., Sect. D: Biol. Crystallogr.* **2007**, *63*, 295−301.
(28) Waugh, D. S. An Overview of Enzymatic Reagents for the Removal of Affinity Tags. *Protein Expression Purif.* **2011**, *80*, 283−293.
(29) Westra, D. F.; Welling, G. W.; Koedijk, D. G. A. M.; Scheffer, A. J.; The, T. H.; Welling-Wester, S. Immobilised Metal-Ion Affinity Chromatography Purification of Histidine-Tagged Recombinant Proteins: A Wash Step with a Low Concentration of EDTA. *J. Chromatogr., Biomed. Appl.* **2001**, *760*, 129−136.
(30) Maret, W. Metalloproteomics, Metalloproteomes, and the Annotation of Metalloproteins. *Metallomics* **2010**, *2*, 117−125.
(31) Liu, J.; Spulber, M.; Wu, D.; Talom, R. M.; Palivan, C. G.; Meier, W. Poly(*N*-Isopropylacrylamide-Co-Tris-Nitrilotriacetic Acid Acrylamide) for a Combined Study of Molecular Recognition and Spatial Constraints in Protein Binding and Interactions. *J. Am. Chem. Soc.* **2014**, *136*, 12607−12614.
(32) Mattiasson, B.; Kumar, A.; Ivanov, A. E.; Galaev, I. Y. Metal-Chelate Affinity Precipitation of Proteins Using Responsive Polymers. *Nat. Protoc.* **2007**, *2*, 213−220.
(33) Luchini, A.; Geho, D. H.; Bishop, B.; Tran, D.; Xia, C.; Dufour, R. L.; Jones, C. D.; Espina, V.; Patanarut, A.; Zhou, W.; Ross, M. M.; Tessitore, A.; Petricoin, E. F.; Liotta, L. A. Smart Hydrogel Particles: Biomarker Harvesting: One-Step Affinity Purification, Size Exclusion, and Protection against Degradation. *Nano Lett.* **2008**, *8*, 350−361.
(34) O'Brien, J.; Shea, K. J. Tuning the Protein Corona of Hydrogel Nanoparticles: The Synthesis of Abiotic Protein and Peptide Affinity Reagents. *Acc. Chem. Res.* **2016**, *49*, 1200−1210.
(35) Casolaro, M.; Paccagnini, E.; Mendichi, R.; Ito, Y. Stimuli-Responsive Polymers Based on L-Phenylalanine Residues: Protonation Thermodynamics of Free Polymers and Cross-Linked Hydrogels. *Macromolecules* **2005**, *38*, 2460−2468.
(36) Malkoch, M.; Thibault, R. J.; Drockenmuller, E.; Messerschmidt, M.; Voit, B.; Russell, T. P.; Hawker, C. J. Orthogonal Approaches to the Simultaneous and Cascade Functionalization of Macromolecules Using Click Chemistry. *J. Am. Chem. Soc.* **2005**, *127*, 14942−14949.
(37) Debord, J. D.; Lyon, L. A. Synthesis and Characterization of pH-Responsive Copolymer Microgels with Tunable Volume Phase Transition Temperatures. *Langmuir* **2003**, *19*, 7662−7664.
(38) Yoshimatsu, K.; Koide, H.; Hoshino, Y.; Shea, K. J. Preparation of Abiotic Polymer Nanoparticles for Sequestration and Neutralization of a Target Peptide Toxin. *Nat. Protoc.* **2015**, *10*, 595−604.
(39) Weisman, A.; Chen, Y. A.; Hoshino, Y.; Zhang, H.; Shea, K. Engineering Nanoparticle Antitoxins Utilizing Aromatic Interactions. *Biomacromolecules* **2014**, *15*, 3290−3295.
(40) Sundberg, L.; Porath, J. Preparation of Adsorbents for Biospecific Affinity Chromatography: I. Attachment of Group-Containing Ligands to Insoluble Polymers by Means of Bifunctional Oxiranes. *J. Chromatogr. A* **1974**, *90*, 87−98.
(41) Nonlinear Least Squares Curve Fitting. http://www.colby.edu/chemistry/PChem/scripts/lsfitpl.html (accessed Mar 13, 2021).
(42) Hoshino, Y.; Urakami, T.; Kodama, T.; Koide, H.; Oku, N.; Okahata, Y.; Shea, K. J. Design of Synthetic Polymer Nanoparticles That Capture and Neutralize a Toxic Peptide. *Small* **2009**, *5*, 1562−1568.
(43) Yoshimatsu, K.; Yamazaki, T.; Hoshino, Y.; Rose, P. E.; Epstein, L. F.; Miranda, L. P.; Tagari, P.; Beierle, J. M.; Yonamine, Y.; Shea, K.

https://doi.org/10.1021/acs.biomac.1c00119
Biomacromolecules 2021, 22, 1695−1705

J. Epitope Discovery for a Synthetic Polymer Nanoparticle: A New Strategy for Developing a Peptide Tag. *J. Am. Chem. Soc.* **2014**, *136*, 1194−1197.
(44) Culver, H. R.; Sharma, I.; Wechsler, M. E.; Anslyn, E. V.; Peppas, N. A. Charged Poly(*N*-Isopropylacrylamide) Nanogels for Use as Differential Protein Receptors in a Turbidimetric Sensor Array. *Analyst* **2017**, *142*, 3183−3193.
(45) Panganiban, B.; Qiao, B.; Jiang, T.; DelRe, C.; Obadia, M. M.; Nguyen, T. D.; Smith, A. A. A.; Hall, A.; Sit, I.; Crosby, M. G.; Dennis, P. B.; Drockenmuller, E.; Olvera de la Cruz, M.; Xu, T. Random Heteropolymers Preserve Protein Function in Foreign Environments. *Science* **2018**, *359* (6381), 1239−1243.
(46) Kaufmann, M.; Lindner, P.; Honegger, A.; Blank, K.; Tschopp, M.; Capitani, G.; Plückthun, A.; Grütter, M. G. Crystal Structure of the Anti-His Tag Antibody 3D5 Single-Chain Fragment Complexed to Its Antigen. *J. Mol. Biol.* **2002**, *318*, 135−147.
(47) Hoshino, Y.; Ohashi, R. C.; Miura, Y. Rational Design of Synthetic Nanoparticles with a Large Reversible Shift of Acid Dissociation Constants: Proton Imprinting in Stimuli Responsive Nanogel Particles. *Adv. Mater.* **2014**, *26*, 3718−3723.
(48) Hoshino, Y.; Miyoshi, T.; Nakamoto, M.; Miura, Y. Wide-Range pKa Tuning of Proton Imprinted Nanoparticles for Reversible Protonation of Target Molecules via Thermal Stimuli. *J. Mater. Chem. B* **2017**, *5*, 9204−9210.
(49) Moreira, I. S.; Fernandes, P. A.; Ramos, M. J. Hot Spots—A Review of the Protein−Protein Interface Determinant Amino-Acid Residues. *Proteins: Struct., Funct., Genet.* **2007**, *68*, 803−812.
(50) Bogan, A. A.; Thorn, K. S. Anatomy of Hot Spots in Protein Interfaces11Edited by J. Wells. *J. Mol. Biol.* **1998**, *280*, 1−9.
(51) Bignotti, F.; Penco, M.; Sartore, L.; Peroni, I.; Mendichi, R.; Casolaro, M.; D'Amore, A. Synthesis, Characterisation and Solution Behaviour of Thermo- and pH-Responsive Polymers Bearing L-Leucine Residues in the Side Chains. *Polymer* **2000**, *41*, 8247−8256.
(52) Bauri, K.; Nandi, M.; De, P. Amino Acid-Derived Stimuli-Responsive Polymers and Their Applications. *Polym. Chem.* **2018**, *9*, 1257−1287.
(53) Oya, T.; Enoki, T.; Grosberg, A. Y.; Masamune, S.; Sakiyama, T.; Takeoka, Y.; Tanaka, K.; Wang, G.; Yilmaz, Y.; Feld, M. S.; Dasari, R.; Tanaka, T. Reversible Molecular Adsorption Based on Multiple-Point Interaction by Shrinkable Gels. *Science* **1999**, *286*, 1543−1545.
(54) Hoshino, Y.; Koide, H.; Furuya, K.; Haberaecker, W. W.; Lee, S.-H.; Kodama, T.; Kanazawa, H.; Oku, N.; Shea, K. J. The Rational Design of a Synthetic Polymer Nanoparticle That Neutralizes a Toxic Peptide in Vivo. *Proc. Natl. Acad. Sci. U. S. A.* **2012**, *109*, 33−38.
(55) Lindner, P.; Bauer, K.; Krebber, A.; Nieba, L.; Kremmer, E.; Krebber, C.; Honegger, A.; Klinger, B.; Mocikat, R.; Plückthun, A. Specific Detection of His-Tagged Proteins with Recombinant Anti-His Tag ScFv-Phosphatase or ScFv-Phage Fusions. *BioTechniques* **1997**, *22*, 140−149.
(56) Kolb, H. C.; Finn, M. G.; Sharpless, K. B. Click Chemistry: Diverse Chemical Function from a Few Good Reactions. *Angew. Chem., Int. Ed.* **2001**, *40*, 2004−2021.

https://doi.org/10.1021/acs.biomac.1c00119
Biomacromolecules 2021, 22, 1695−1705